Optimization of Graphene Oxide through Various Hummers' Methods and Comparative Reduction using Green Approach.

[1]Allen Abiodun Olorunkosebi,[1]Marcus Adebola Eleruja,[2]Adetayo Victor Adedeji,[1*]Bolutife Olofinjana,[1]Oladepo Fasakin,[1]Ezekiel Omotoso,[3]Kabir Oyeniran Oyedotun,[1]Ezekiel Oladele Bolarinwa Ajayi,[3]Ncholu Manyala.

[1]Department of Physics and Engineering Physics, Obafemi Awolowo University, Ile-Ife, 220005, Nigeria

[2]Department of Chemistry and Physics, Elizabeth City University, Elizabeth City, NC, USA

[3]Department of Physics, Institute of Applied Materials, SARChI in Carbon Technology and Materials, University of Pretoria, Pretoria 0002, South Africa

*Corresponding Author Tel: +234 8066762570, E-mail address: olofinb@oauife.edu.ng

Abstract

Graphene oxide (GO) was synthesized using three techniques and was reduced using two reducers' extracts from neem and pumpkin leaves. The obtained GOs and RGOs were characterized using Fourier infra-red (FTIR) spectroscopy, Raman spectroscopy, UV-visible spectrophotometry, energy dispersive x-ray spectroscopy (EDX) and scanning electron microscopy (SEM). Results revealed that all the three methods used are capable of producing GO with various levels of oxidation. FTIR spectra of RGOs showed that the C=O signature of GOs at 1730 - 1740 cm^{-1} were eliminated after reduction. Other characterization results of the RGOs revealed that both the neem and pumpkin extracts are capable of reducing the synthesized GO. With all these, it can be concluded that the extracts of neem and pumpkin are good reducing agents. The neem and pumpkin extracts, which are ecofriendly can replace the use of hazardous chemicals that are not ecofriendly.

Keywords: Graphite; Graphene oxide; Reduced graphene oxide; Neem; Pumpkin

1.0 Introduction

In recent time, graphene has been widely studied due to its promising applications in engineering and medicine [1-4]. It has produced an excellent application in the field of thin film electronics, touch screen, p–n junction materials, flexible thin-film transistors, solar cells optoelectronics, energy storage and various types of sensors [4-6]. This is as a result of its exceptional optical, mechanical, heat and electrical properties [5-7]. This called for an urgent cheaper and safer ways of synthesizing graphene for large scale production that will be similar to natural graphene.

The most widely used method for synthesizing graphene oxide (GO) is the Hummers' method which has been used since 1958 [8]. The method is less hazardous as potassium permanganate ($KMnO_4$) was used instead of potassium chlorate ($KClO_3$), as oxidizing agent [9]. Various modifications have been introduced to the Hummers' method in the process of oxidation, in order to improve the quality of GO, save time and make the process more ecofriendly which has led to; modified Hummers method, improved Hummers method, simplified Hummers method [9-13], among others.

Over the years, several techniques have been used to reduce graphene oxide with cost effective and bulk production being the main objective [14] Reduced graphene oxide has similar mechanical, optoelectronic or conductive properties to pristine graphene because it possesses a heterogeneous structure comprised of a graphene-like basal plane that is additionally decorated with structural defects and populated with areas containing oxidized chemical groups [15]. Various chemical methods have been used extensively [15-16]. Most of the reducing agent used in the chemical methods such as hydrazine monohydrate, hydroquinone and sodium borohydride are hazardous and can cause various types of harm to human and environment. They are poisonous when inhaled and corrosive to skin. In view of this, scientists are gradually tending towards methods that are cost-effective, less hazardous

and environmentally friendly. This includes, the use of plant extracts rich in antioxidant that can be used as reducing agent, vitamin C and amino acid [16].

There are so many leaves of plants around us which contain reducing agents such as flavonoid, tannin, alkaloid, amino acid, and vitamin C [17]. Neem with botanical name of *Azadirachta indica*, is a green plant that is common nearly everywhere in the world [18]. The phytochemical screening shows the presence of alkaloids, steroids, tannins, amino acid, flavonoid and saponins [19-21]. Pumpkin with a botanical name of *Telfairia occidentalis,* is another plant in which the phytochemical screening shows that alkaloids, flavonoids, saponins, tannins, terpenoids and amino acid are present [22].

In this study, GO was synthesized using three approaches in Hummers' method: modified Hummers' method for ecofriendly GO; improved modified Hummers method for cost reduction process by removal of a particular chemical; and simplified modified Hummer' method for fast method in the production of GO. An attempt was also made to use the extracts of two plants - neem and pumpkin, as reducing agents in order to overcome environmental and health hazard posed by harmful hydrazine monohydrate and other harmful reducing agents.

2.0 Experimental Techniques

2.1 Synthesis of Graphene Oxide (GO)

2.1.1 Modified Hummers' Method

A mixture of 1.5 g of graphite (44 μm, 99.8% carbon, ash color from Asbury Carbon, New Jersey, USA; Sulphuric acid (98%), Phosphoric acid (85%), Potassium permanganate (99%), were purchased from Sigma). and 9 g of $KMnO_4$, was added gradually into a conical flask containing 200 mL mixture of H_2SO_4 and H_3PO_4 in ratio 9:1, placed in an ice bath and was continuously stirred until a suspension was formed while keeping the temperature below 20 ºC. The suspension was then transferred to a hot plate with magnetic stirrer at temperature

of 50 ºC and stirred continuously for 11 hours. 500 mL of deionized water was added to the suspension, and after 5 minutes, 20 mL of hydrogen peroxide (H_2O_2) was also added dropwisely to stop the oxidation reactions. This was then centrifuged to remove the solid part of the suspension and later washed with 5% HCl repeatedly. Deionized water was then used to wash the resulting paste until the pH was 7. Finally, the product was oven dried at 60 ℃ and milled into powder form. The process was repeated while the stirring period (oxidation time) was also extended to 12, 13 and 14 hours. Samples were labeled according to the stirring period as GO11H, GO12H, GO13H and GO14H respectively for easy identification.

2.1.2 Modified Hummers' Method without Phosphoric Acid

This method is similar to that of modified Hummers' method reported above in terms of chemical used but an adjustment was made to the constituents by removing H_3PO_4. Mixture of graphite powder (2.0 g) and $KMnO_4$ (9.0 g) was added gradually into H_2SO_4 (70 mL) in a conical flask and was continuously stirred in an ice bath until a suspension was formed while keeping the temperature below 20 ºC, as the reaction is exothermic. The conical flask containing the suspension was then transferred to a hot plate with magnetic stirrer at temperature of 50 ºC and stirred vigorously for about 30 minutes. Later, 150 mL of deionized water was added, and the suspension was stirred for another 15 minutes at 95 ºC. After the whole process, 500 mL deionized water was added to dilute the suspension, followed by a dropwise addition of 15 mL of H_2O_2 to terminate any further oxidation. The suspension was centrifuged to remove the solid part of the suspension and later washed with 5% HCl repeatedly. Deionized water was then used to wash the paste until the pH was 7. Finally, product was oven dried at 60 ℃ and milled into powder. The sample was tagged GONP.

2.1.3 Simplified Hummers' Method

Mixture of 1.0 g of graphite and 0.6 g of $NaNO_3$ was dissolved in 23 mL of H_2SO_4 and cooled in an ice bath with rapid stirring keeping the temperature below 20 ºC. 3.0 g of

$KMnO_4$ was then added gradually while stirring. After 15 minutes, the flask containing suspension was taken into a water bath at temperature of 35 ^oC and continuously stirred for 30 minutes. Later, 30 mL of deionized water was gently added to the suspension and stirred for one hour. After this process, the suspension was diluted with 30 mL of deionized water. Then, 3 mL of hydrogen peroxide (H_2O_2) was added into the suspension to terminate the oxidation. The suspension was centrifuged to remove the solid part of the suspension and later washed with 5% of HCl repeatedly. Deionized water was then used to wash the product until the pH was 7. Finally, the product was oven dried at 60 ^oC and milled into powder form and labelled as GOSIM.

2.2 Synthesis of Reduced Graphene Oxide (RGO).

2.2.1 Preparation of Green Extracts.

Neem leaves were washed separately for several times with distilled water. 250 g the neem leaves was mixed with 1 L of distilled water and heated at 90 ^oC for 10 minutes until the water had turned green. After cooling down to room temperature, the extract was filtered using Whitman filter paper number one and kept in a refrigerator. The process was also repeated for pumpkin leaves.

2.2.2 Reduction of Graphene Oxide using Extracts from Neem Leaves and Pumpkin Leaves

Before the reduction process, optimization was done for GO11H, GO12H, GO13H and GO14H, after which only GO12H was chosen for the reduction. In a typical reduction experiment, dried sample of GO12H, GONP and GOSIM were each added to distilled water to form a suspension. 700 mg of GO12H was added to 1400 mL of distilled water, 250 mg of GOSIM to 500 mL of distilled water and 250 mg of GONP to 500 mL of distilled water. Each suspension was stirred vigorously for 30 minutes on a magnetic stirrer heated at 30 ^oC. 140 mL of Neem extract was added to GO12H suspension, while 50 mL was added to each of GONP and GOSIM suspensions. Each of these were kept in a tightly sealed glass bottle and

stirred at 30 ºC for 24 hours to obtain a homogeneous suspension. The time is in accordance with other reducing agents: Hydrazine for 24h at 100^{O}C [23]; Alaline with reduction time of 24h [24]. Then, the suspension was centrifuged at 4000 rpm and washed severally with distilled water. Finally, a black product was obtained for each of the sample, which was oven-dried at 60 ºC. It was then milled to form a powder and labelled as NRGO12H, NRGONP and NRGOSIM respectively. This process of reduction was repeated for pumpkin extracts and the black powder obtained were labelled PRGO12H, PRGONP and PRGOSIM

2.3 Characterization of Samples

The Fourier-transform infrared spectroscopy (FTIR) analysis of the starting material (graphite), GO and RGO was carried out using SHIMADZU FTIR model 8400S spectrophotometer. UV-visible analysis of samples was done using UV-visible spectrophotometer (SHIMADZU Model 6405) with quartz as a cuvette and distilled water was used as a solvent to dissolve all the samples. The Raman spectroscopy analysis was carried out using Wintec-alpha 300R^{+} confocal Raman spectrometer (WinTech GmbH). The laser source used has wavelength of 532 nm and energy of 2.33 eV, through a numerical aperture of 0.9 and 100x magnification of the spectrometer. Surface morphology of GOs and RGOs was observed under scanning electron microscope (SEM, JEOL JSM-6010 PLUS/LA) while elemental composition was determined using energy dispersive X-ray spectroscopy (EDX) incorporated with the scanning electron microscope (SEM).

3.0 RESULTS AND DISCUSSION

3.1 Graphene Oxide

3.1.1 Fourier Transform Infrared Spectroscopy Analysis of Graphite and GOs.

The FTIR analysis gives the qualitative properties of oxygen containing group in the GO spectrum [25]. Figure 1a shows spectrum for graphite and GO11H, GO12H, GO13H GO14H. In the spectrum of graphite, three prominent peaks were observed: the stretching

and bending vibration of C-OH group at 3437.24 cm^{-1}, COOH group at 2357.42 cm^{-1} and C=C at 1634 cm^{-1} corresponding to the carbon composition of graphite [26-27].The presence of both C-OH, which is the bound of OH to carbon grid and COOH group, is probably as a result of water molecules absorbed from the atmospheric exposure and hydrogen of unextractable water molecule forming a bound as C-OH and COOH, [26, 28]. When the spectrum for graphite was compared with that of the GOs, the stretching and bending vibration of C-OH group were also observed for all GO variants at 3415.60 cm^{-1} - 3419.90 cm^{-1}. At the middle of the spectra for GOs, a pair of bands was observed, which is the vibration at 1730 - 1740 cm^{-1} with the stretching modes of C=O bond and vibration at 1630-1650 cm^{-1}, the stretching modes of C=C bond that was originated from unoxidized sp^2 carbon bond. The stretching modes of C=O bonds is generally termed as the signature of GO, the evidence that graphite had been oxidized [29]. When the intensity of the C=O bonds for GO11H, GO12H, GO13H and GO14H were compared, it increased from GO11H to GO12H, but with no significant changes when the oxidation time was increased beyond 12 hours (that is for GO13H and GO 14H). This implies that the concentration of oxygen at GO11H increased as the time of oxidation increases, and optimized after 12 hours of stirring for GO12H. In the spectra, signature of GO, was also present in GONP and GOSIM (Figure 1b). When the intensities of GO signature, (the C=O stretching vibration 1730 - 1740 cm^{-1}) were compared, GO11H, GO12H, GO13H, GO14H exhibited high level of oxidation, followed by GOSIM and then, GONP. In all, GO was synthesized in all the three approaches with various level of oxidation.

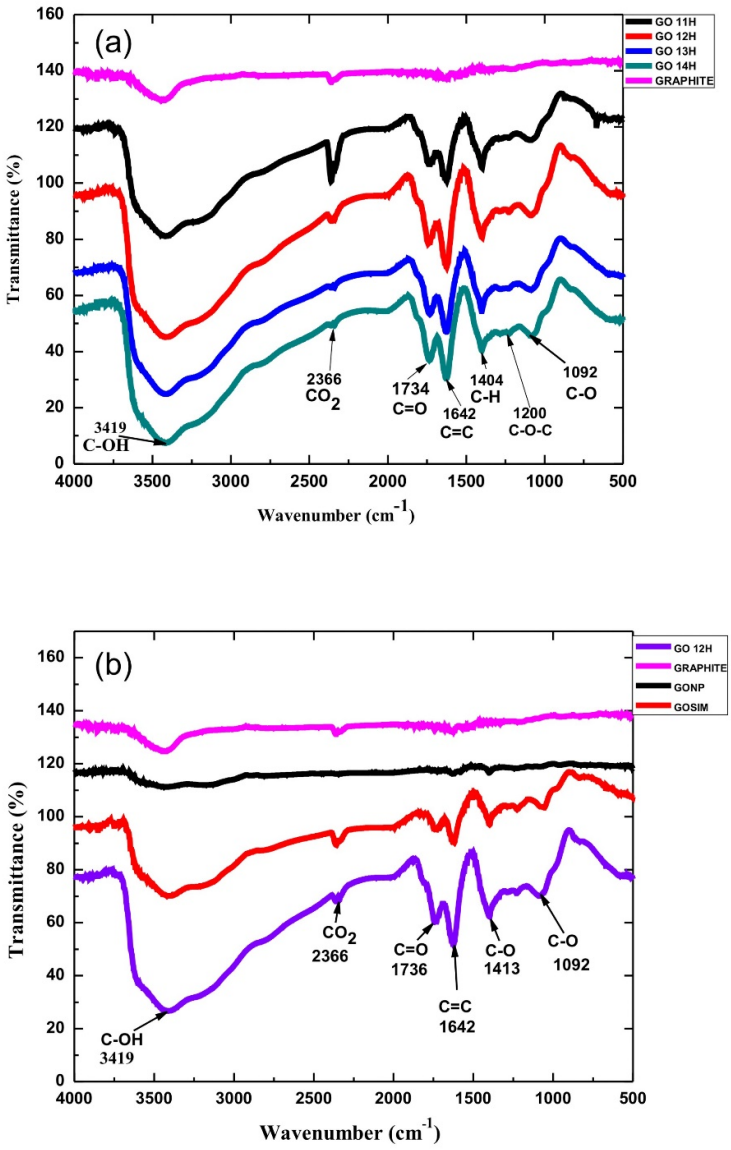

Figure 1: FTIR Spectrum of (a) GO11H, GO12H, GO13H and GO14H compared with graphite. (b) GO12H, GONP and GOSIM compared with graphite.

3.1.2 Raman Spectral Analysis of GOs Powder

Generally, Raman spectrum of any graphene-based materials are characterized by two main features, the D and G bands. The D band (at Raman shift of 1350 cm^{-1}) represents the breathing mode of aromatic rings as a result of defect in the samples during oxidation [30,31] while the G band (at Raman shift of 1575 cm^{-1}), emanated from first-order scattering of E_{2g} phonons by sp^2 atom ring, which arises from a breathing mode of j-point photons of A_{1g} symmetry [32]. Figure 1 is the Raman spectrum of as-received graphite and it is the standard for all other prepared samples which only displayed the G band at 1575 cm^{-1}. While in Figure

2, the G band of each synthesized GO was broadened and shifted to 1596 $cm^{-1}$for GO 11H, 1594 cm^{-1} for GO12H, 1592 $cm^{-1}$for GO13H and GO14H, 1586cm^{-1} for GONP, and 1579 cm^{-1} for GOSIM. The D band was observed at 1350 cm^{-1} for GO11H, GO13H and GO14H; and1357 cm^{-1} for GO12H. It was shifted to a lower region (1347 cm^{-1}) for GONP and 1348 cm^{-1} for GOSIM, indicating the destruction of sp^2 character and the formation of defects in the sheets due to extensive oxidation. Similar result was obtained by Kudin *et al*. (2008) [33].

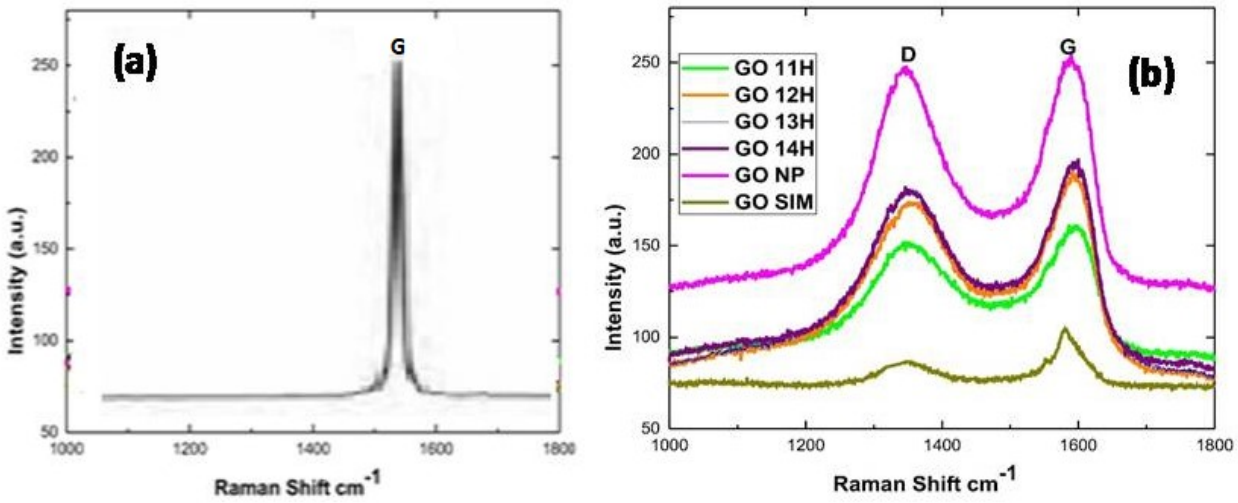

Figure 2: (a) Raman spectrum of Graphite (b) Raman spectra of GO11H, GO12H, GO13H, GO14H, GOSIM and GONP

The intensity ratio of the D band to the G band in Raman spectra measures the average size of sp^2 domain as well as the degree of disorderliness [34]. Using Tuinstra–Koenig relation, the I_D/I_G ratio is inversely proportional to the crystal size (L_D) of sp^2 domain, [35].

$$\frac{I_D}{I_G} = \frac{C'(\lambda)}{L_D}$$

$$L_D = C'(\lambda)\left(\frac{I_D}{I_G}\right)^{-1} \qquad (1)$$

Where, $C'(\lambda)$is the fourth power of the laser wavelength, which is given by

$C'(\lambda) = (2.4\ x\ 10^{-10}\ nm^{-3})\ \lambda^4$[36], λ= Raman excitation wavelength.

Table 1 summarizes the intensity ratio of the respective GOs. For the GOs prepared using the modified Hummers' method, there is a reduction in the intensity ratio from 0.938 to 0.915 as the time of oxidation increased from 11 to 14 hours. This shows an increase in crystal size as the degree of oxidation increases [37]. However, the value of intensity ratio, I_D/I_G for GO12H, GO13H and GO14H produced no significant changes. From the table, the intensity ratio of GONP is 0.959, while that of GOSIM is 0.831. This implies that there was an extensive vibration of crystalline structure leading to the formation of defect with an increase in crystal size [38-39].The values of the I_D/I_G ratio obtained is similar to what has been obtained in the literature [38-40].

Table 1: Intensity ratio (I_D/I_G) of GOs

Sample	D band (cm^{-1})	I_D	G band (cm^{-1})	I_G	I_D/I_G
GO11H	1350.66	151.73	1596.66	161.69	0.938
GO12H	1357.44	172.90	1594.30	187.94	0.920
GO13H	1352.72	180.42	1592.53	196.70	0.917
GO14H	1350.66	180.63	1592.59	197.34	0.915
GONP	1347.10	244.23	1586.94	254.94	0.959
GOSIM	1348.37	86.60	1579.70	104.24	0.831

3.1.3 Optical Characterization of GO

Optical analysis of any graphene-based material can manifest an exciting absorption patterns at the wavelength regions of approximately 230 nm and 300 nm, which correspond to transitions involvingπ - π*transition of the aromatic C=C and n - π*transition of the C=O electrons band energies [41]. Figure 3a shows a characteristic peak at approximately 231 nm corresponding to π - π*band for all GOs synthesized. This is attributed to π - π* plasmon of the C=C bonds which was inherited from graphite. Another shoulder peak observed at approximately 302 nm was observed for GO11H, GO12H, GO13H and GO14H.This was attributed to n - π* plasmon of the C=O bonds, which suggested that the materials were oxidized. Similar results were also reported by Cao and Emadi (2012) [42]. The value of n -

π* plasmon for GOSIM is 309.48 nm, while that of GONP is 308.56 nm. Energy band gap graph in Figure 3c shows the plot of square of absorption coefficient (α^2) against the energy of the photon for all GOs. The analysis of the results revealed an energy band gap (E_g) increase from GO11H (2.23 eV) to GO12H (2.57 eV). Subsequently, the value began to reduce for GO13H (2.35 eV) and GO14H (2.14 eV). GOSIM energy band gap value is approximately closed with GO12H at 2.57 eV. GONP energy band gap gave the highest value of 2.72 eV. These different values obtained may be attributed to the process of oxidation. Table 2 shows the UV analysis of all GOs.

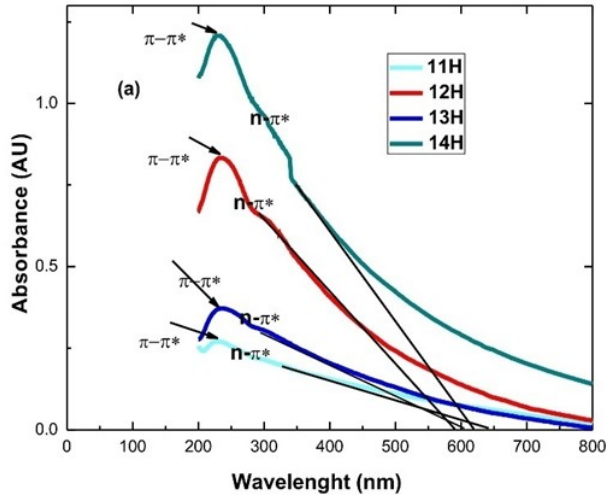

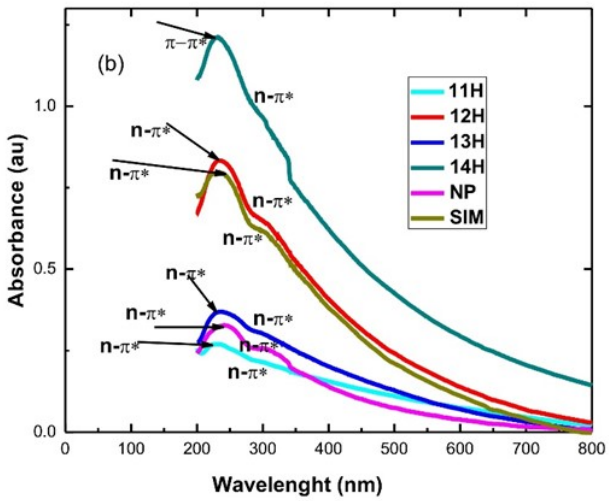

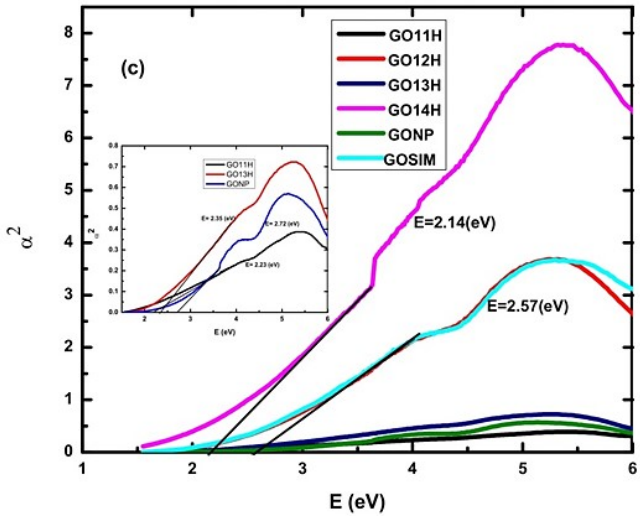

Table 2: UV analysis of GOs

Sample	π-π* (nm)	n-π* (nm)	E_g (eV)
GO11H	231.59	302.89	2.23
GO12H	231.19	302.7	2.57
GO13H	231.15	302.7	2.35
GO14H	231.15	302.71	2.14
GONP	231.45	308.56	2.72
GOSIM	231.59	309.48	2.57

3.1.4 Scanning Electron Microscopy Analysis of Graphite and GOs Powder

From the FTIR result, when the level of the intensity of C=O signature of stretching vibration (1730 - 1740 cm^{-1}) peaks for GO11H, GO12H, GO13H and GO14H were compared, there was an increase in value from GO11H to GO12H, but no significant change in GO12H, GO13H and GO14H. Also, from Raman spectra, the I_D/I_G ratio for GO12H, GO13H and GO14H show no significant changes, compared to that of GO11H to GO12H. The optical analysis also shows that, n - π* plasmon of the C=O bond nm for GO11H, GO12H, GO13H and GO14H were observed at approximately the same wave number, 302nm. As a result, for further characterization, GO12H was chosen as a representation of the GOs from GO11H, GO12H, GO13H and GO14H, along with GONP and GOSIM.

The SEM micrographs of the graphite and synthesized GOs are given in Figure 4. Figure 4a shows the micrograph of graphite as received. The flake shape is clearly visible at the edges and exhibited multiple layers arranged on top of one another. Each sheet can also be identified from their edges. A similar observation was also reported by Badenhorst (2017), [43]. For GO12H in Figure 4b, there is an ultra-thin layer with folded edges, showing a surface which appeared to be continuous. Individual sheet can be clearly differentiated through the edges, with wrinkled and kinked areas. They are intercalated with roughed surfaces, which is the result of structural deformation upon exfoliation and restacking. This was also observed by Gurunathan *et al*., (2013) [44]. This is similar to that of GOSIM in Figure 4d with a slight difference due the level of oxidation. For GONP in Figure 4c, there is a structure at the center which is similar to that of graphite in Figure 4a, which may be attributed to the level of oxidation.

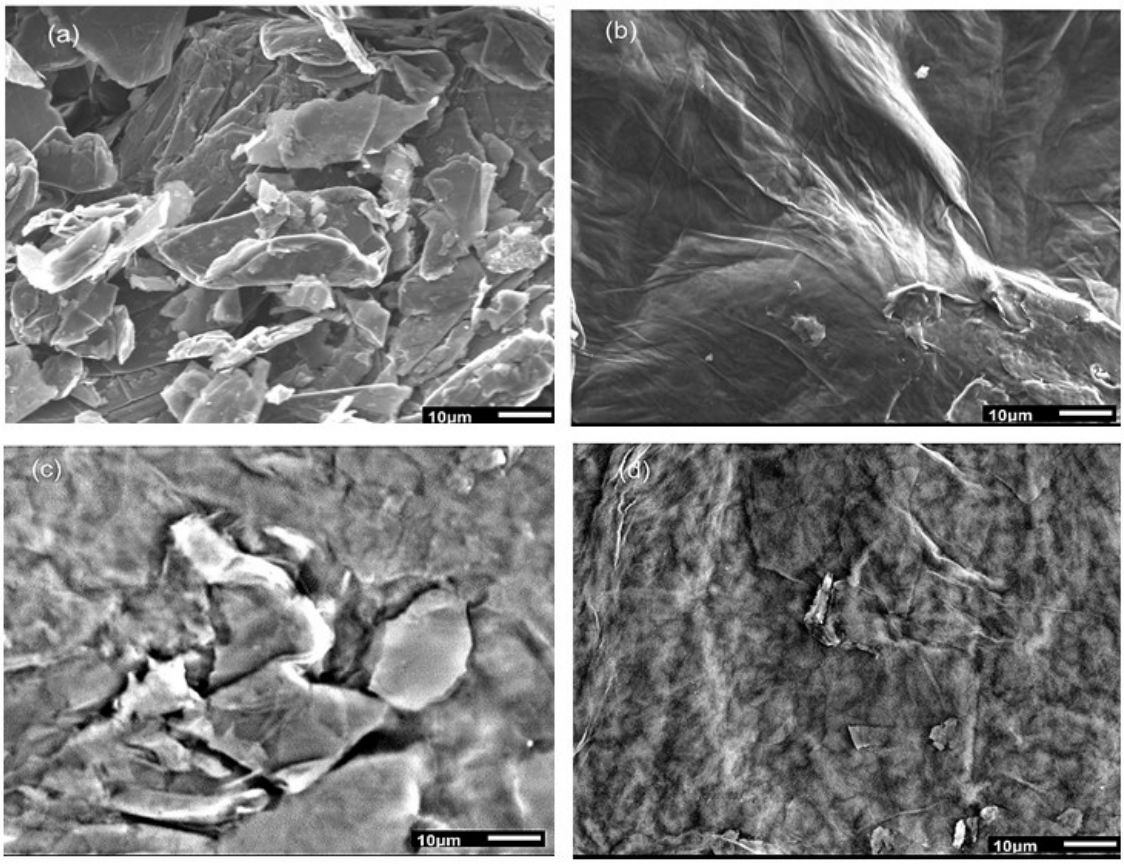

Figure 4: SEM Micrograph of (a) Graphite (b) GO12H (c) GONP (d) GOSIM

3.1.5 Energy Dispersive X-Ray Analysis of Graphite and GOs

Figure 5a shows the typical EDX spectrum of the graphite as received, which was used as the starting material. The spectrum revealed the presence of carbon at 99.77% atomic composition, to confirm that graphite is an allotropy of carbon. Figures 5b – 5d show the spectra of GO12H, GONP and GOSIM respectively. Each spectrum shows the presence of carbon and oxygen atoms in various proportion depending on the level of oxidation, thereby confirming the synthesis of GO [43]. From the spectrum in Figure 5b, GO12H contained 43.03% of oxygen to 55.78% of carbon. Figures 5c and 5d indicate that, GOSIM and GONP possessed 36.91% of oxygen to 63.09 % of carbon and32.37% of oxygen to 67.63 % of carbon respectively. When all GOs are compared, the results confirmed that GO12H contain more oxygen followed by GOSIM and then, GONP. The presence of chlorine and sulphur were observed in GOSIM. Cl can be attributed to the HCl used in the washing of the sample, while the presence of sulphur, is as a result of H_2SO_4 used for the oxidation process.

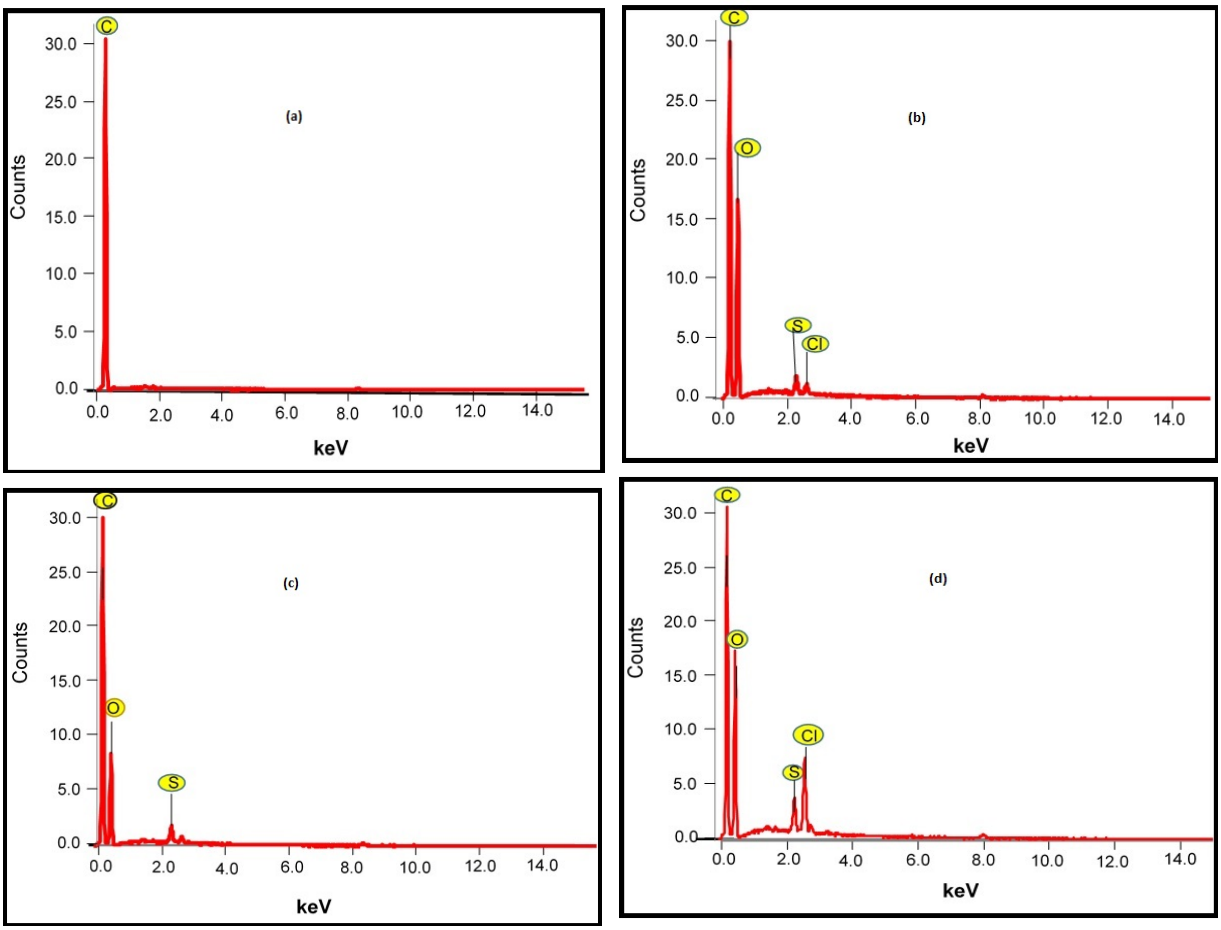

Figure 5: EDX spectrum of (a) Graphite (b) GO12H (c) GONP (d) GOSIM

3.2 Reduced Graphene Oxide (RGO)

GO12H, GONP and GOSIM were selected for reduction using pumpkin and neem extract. Reduction by neem gave rise to NRGO12H, NRGONP and NRGOSIM, while reduction with pumpkin gave rise to PRGO12H, PRGONP and PRGOSIM.

3.2.1 Fourier Transform Infrared Spectroscopy Analysis of RGOs

Figure 6a shows the FTIR spectra of graphite, GO12H, NRGO12H and PRGO12H. Figure 6b shows the spectra of graphite, GONP, NRGONP and PRGONP. Lastly, Figure 6c shows the spectra of Graphite, GOSIM, NRGOSIM and PRGOSIM compared. This was done to compare the spectra of the process of various GOs from graphite and reductions from the two reducers. In all the spectra compared in Figures 6a-c, the stretching and bending

vibration of C-OH groups were still observed in the spectra, but there is a slight reduction in bending of the vibration from 3415.90 cm^{-1} to 3389.29 cm^{-1}. COOH peak appeared again in the spectra of NRGO12H, PRGONP and NRGOSIM in Figures 6a, 6b and 6c respectively. This may be attributed to air exposure after reduction, since it was not peculiar to one reduction method alone. Vibration of C=O of carbonyl groups present at the edges of all GOs has disappeared or diminished in all the RGOs which confirmed that the GO was successfully exfoliated to graphene sheets (RGO). Similar results were also reported by Stankovich *et al*. (2006) [46] and Olumurewa *et al*., (2020) [51]

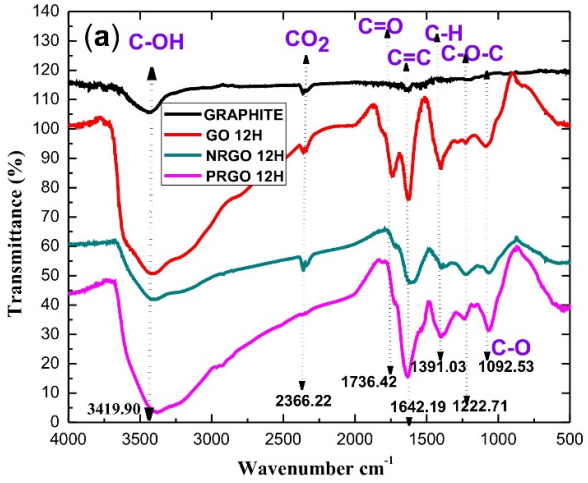

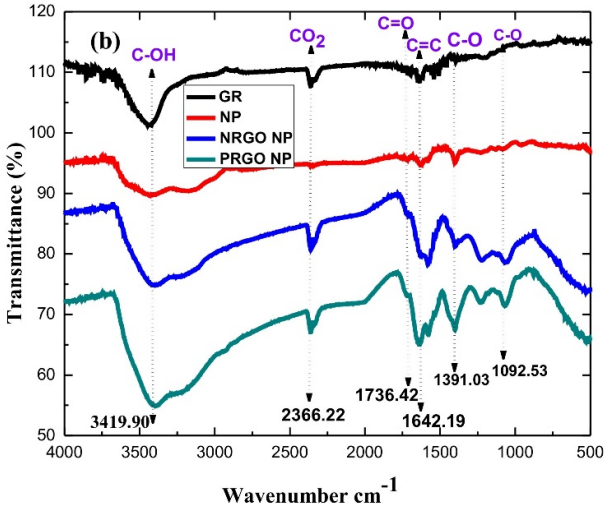

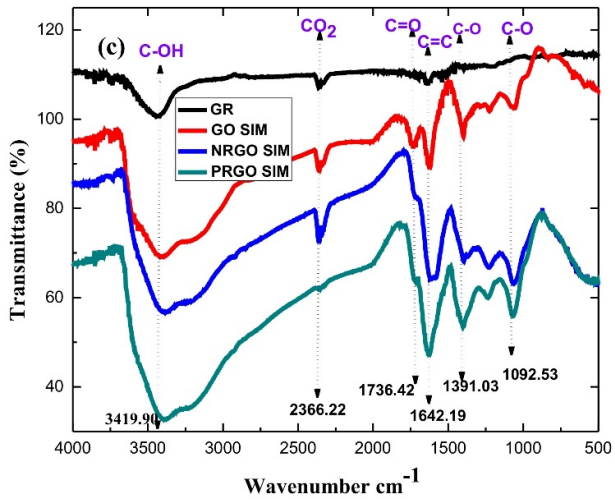

Figure 6: FTIR Spectrum of (a) Graphite, GO12H, NRGO12H and PRGO12H (b) Graphite, GONP, NRGONP and PRGONP (c) Graphite, GOSIM, NRGOSIM and PRGOSIM

3.2.2 Scanning Electron Microscopy Analysis of RGOs

Figures 7a-f show the surface morphology of all RGOs. It can be seen that all the surfaces were more refined and smoother than GOs. In the case of GOs (Figures 4 a-d) curved edges were observed but in all the RGOs sharp edges were observed. This confirmed that graphene oxide had been reduced. Similar result was obtained by Badenhorst (2017) [43]. Moreover, in all the RGO samples, corrugated surface was observed. This was due to the escape of oxygen-containing groups during reduction process [47].

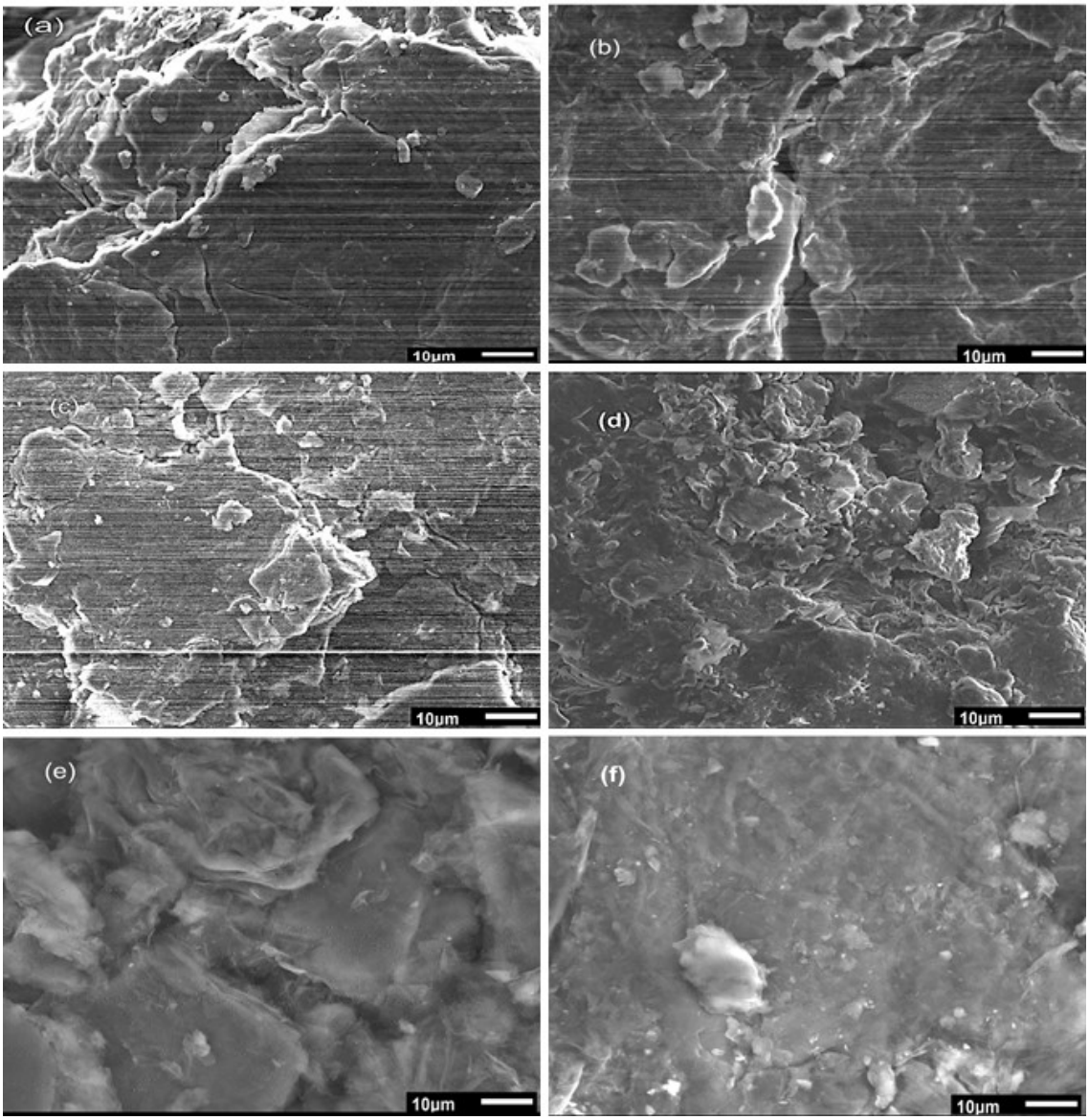

Figure 7: SEM Micrograph of (a) NRGO12H (b) NRGONP (c) NRGOSIM (d) PRGO12H (e) PRGONP (f) PRGOSIM.

3.2.3 Raman Spectral Analysis of RGOs Powder

Figures8(a-c) show the spectra for NRGO12H and PRGO12, NRGONP and PRGONP, NRGOSIM and PRGOSIM. In the Raman spectra, D band occurred at 1351.18 cm^{-1} and

1352.27 cm^{-1}, while G band occurred at 1591.14 cm^{-1}and1589.33 cm^{-1} for NRGO12H and PRGO12H respectively. The reduction in the wavenumber of the D peak towards a lower wavenumber is consistent with previous studies [48, 49]; signifying a considerable reduction of graphene oxide and Sp^2 network restoration. The structural properties of rGO can be observed and analyzed from the relative intensity of the D and G peak of the Raman Spectra [50,51]. There was a Raman shift in NRGO12H and PRGO12H, when compared with GO12H in Table 2. This is as a result of removal of the functional groups, the π surface and structural defects, such as vacancies or rearranged structures of the carbon framework [52]. NRGO12H showed more shift compared to PRGO12H.Similar results were obtained in Figure 8b and 8c. Their respective results are summarized in Table 3. Comparing Table 3 with Table 2, there was an increase in intensity ratios (I_D/I_G) for all RGOs obtained. This can be attributed to the removal of oxygen and restoration of the sp^2 network during the reduction process [53]. The I_D/I_G ratio obtained is similar to what has been obtained earlier, which ranges between 0.9 to 1.0 [42,52-54]. This shows that pumpkin and neem are good reducing agents which can replace the commonly used hazardous chemicals.

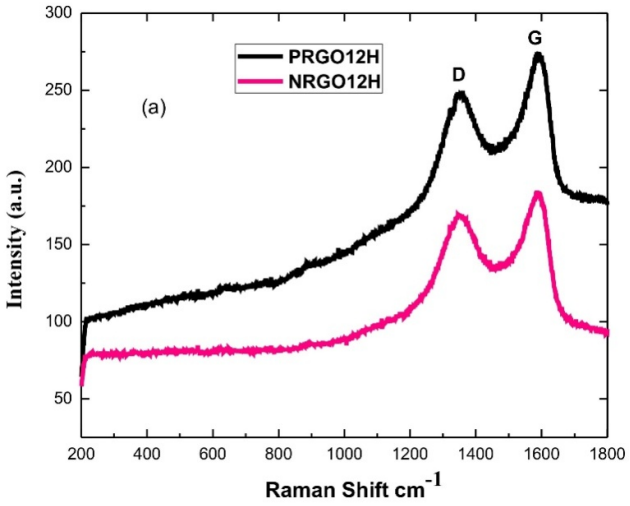

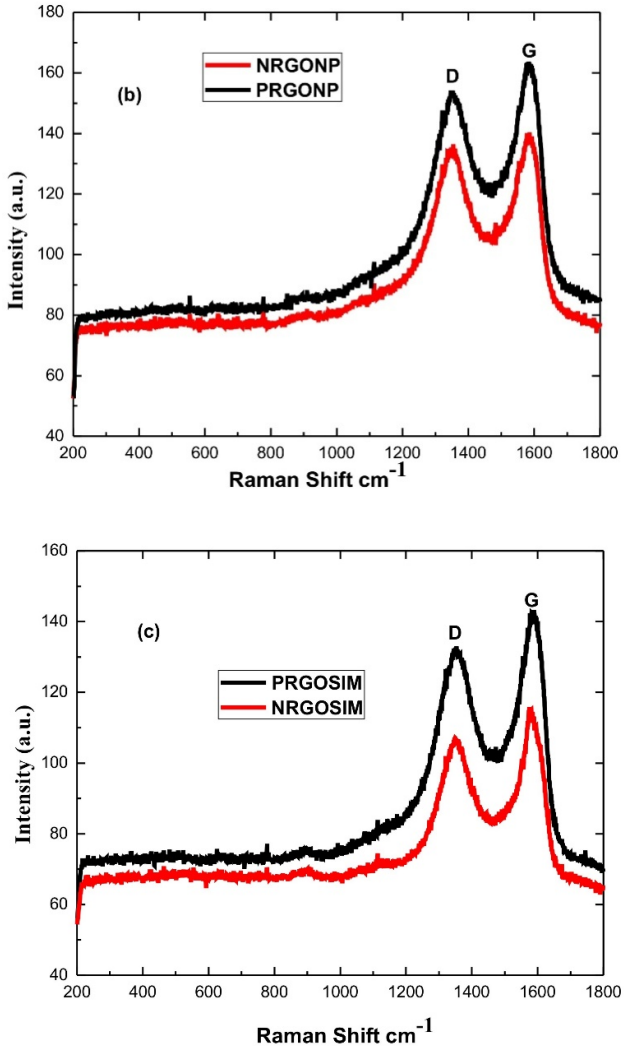

Figure 8: Raman spectrum of (a) NRGO12H and PRGO12H (b) NRGONP and PRGONP (c) NRGOSIM and PRGOSIM

Table3: Intensity ratio (I_D/I_G) of RGOs

Sample	D band (cm^{-1})	I_D	G band (cm^{-1})	I_G	I_D/I_G
NRGO12H	1351.18	169.93	1591.14	183.04	0,925
PRGO12H	1352.27	248.23	1589.33	271.84	0.913
NRGONP	1350.61	134.08	1582.57	141.15	0.950
PRGONP	1351.69	153.51	1582.38	163.37	0.940
NRGOSIM	1350.95	107.07	1577.40	115.05	0.931
PRGOSIM	1350.80	132.34	1584.11	142.47	0.928

3.2.4Optical Characterization of RGOs

Figures 9a and b show plot of absorbance against wavelength for NRGO12H, NRGONP and NRGOSIM; PRGO12H, PRGONP and PRGOSIM. The π - π* plasmon peak of the C=C bond which appeared at approximately 231 nm for GOs, red-shifted to between258 -265nm for RGOs. This is as a result of an increase in π - π* electron concentration and structural ordering, which is consistent with the restoration of sp^2hybridization carbon and possible rearrangement of atoms through reduction [55]. In Table 4, there is a slight increase in the red shifting when neem extract was used for reduction compared to when pumpkin extract was used for reduction. This may be attributed to an increase in π - π* electron concentration, which represent the reduction level between neem and pumpkin extract [56]. The n – π* was also red shifted from 302-309 nm to 337-344 nm, which may be attributed to reduction in sp^3 carbon [50]. Figures 9c and 9d show a plot of direct allowed energy band gap for NRGOs, and PRGOs respectively. Their values experienced an increase in the energy band gap (E_g) which may be attributed to the constituents of the plant used in reductions. The summary of the result is given in Table 4.

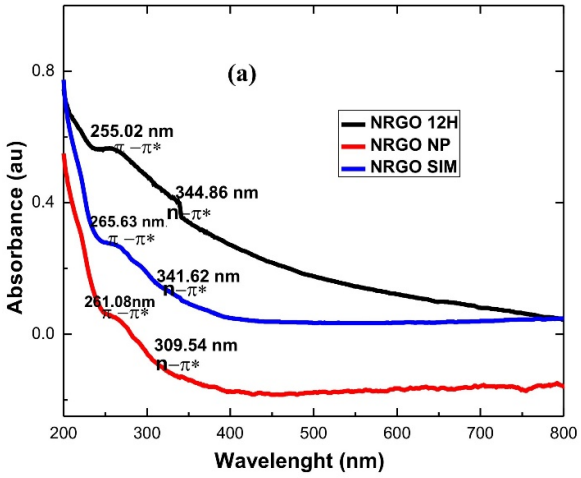

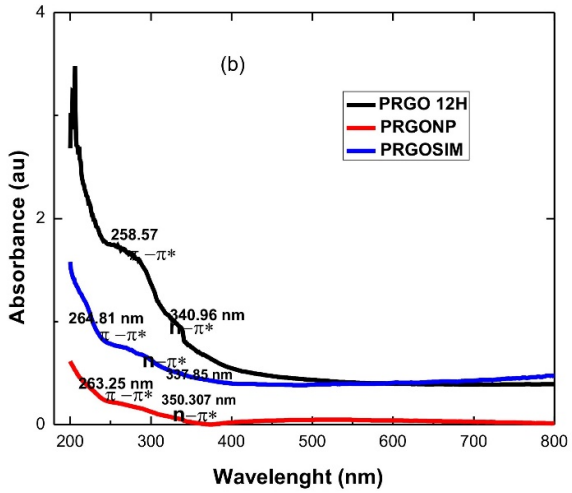

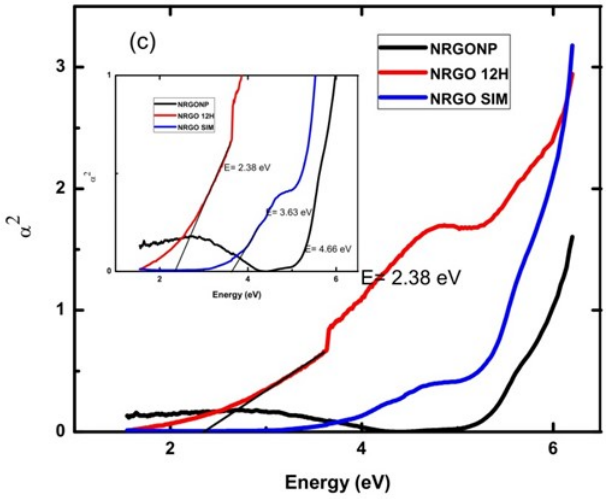

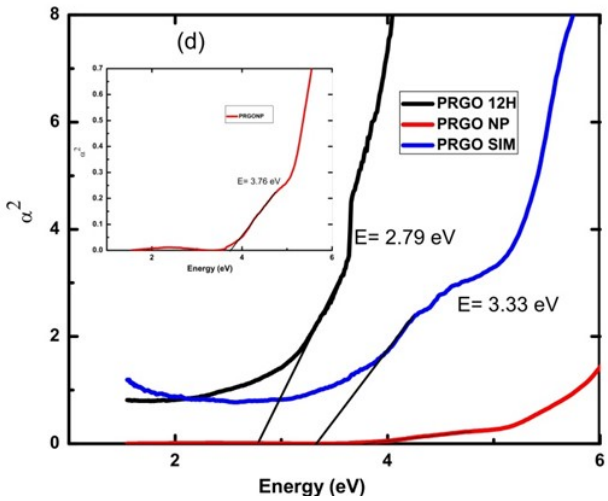

Figure 9: UV Spectrum of Synthesized (a) NRGO12H, NRGONP and NRGO SIM (b) PRGO12H, PRGONP and PRGOSIM; Square of absorption coefficient (α^2) vs. energy of

synthesized (c) NRGO12H, NRGONP and NRGOSIM (d) PRGO12H, PRGONP and PRGOSIM

Table 4: UV analysis of GOs reduced by neem and pumpkin extracts

Sample	π-π* (nm)	n-π* (nm)	E_g (eV)
NRGO12H	265.02	344.86	2.38
NRGONP	265.63	341.86	3.63
NRGOSIM	264.08	341.54	4.66
PRGO12H	258.57	340.96	2.79
PRGONP	264.81	337.85	3.33
PRGOSIM	263.25	350.25	3.76

3.2.5 Energy Dispersive X-Ray Analysis of RGOs

EDX spectroscopy is a tool used in determining the entity and quantity of the elements present in the sample. Figures 10 (a – f) show the spectra of NRGO12H, NRGONP, NRGOSIM, PRGO12H, PRGONP and PRGOSIM. From the spectra analysis, after reduction process, the compositions of carbon content increase while there was reduction in the oxygen content in all the RGOs. For instance, in GO12H, there was a reduction in oxygen contents from 43.07% to 36.00% and 38,60%for NRGO12Hand PRGO12H respectively.

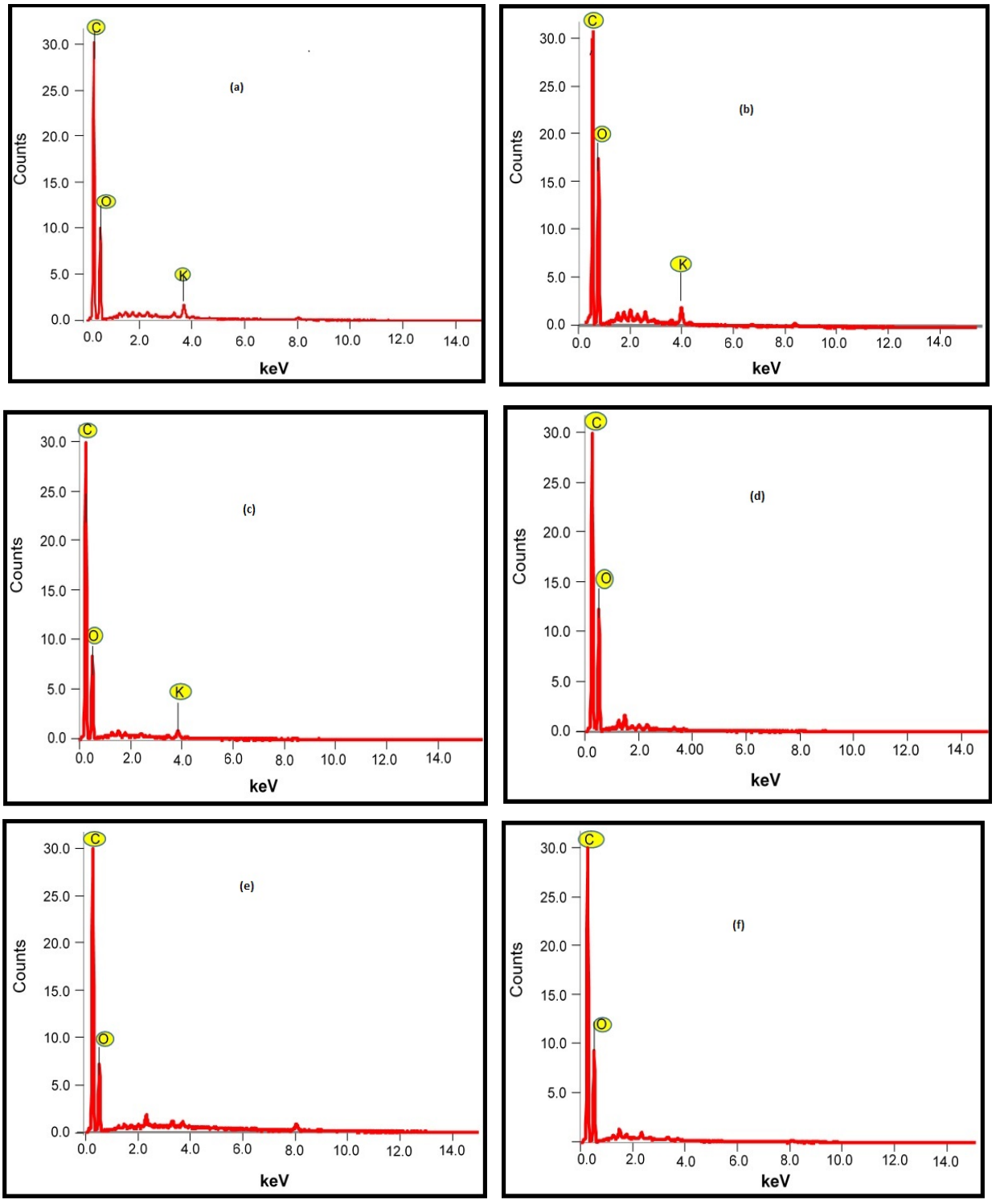

Figure 10: EDX spectrum of (a) NRGO12H (b) NRGONP (c) NRGOSIM (d) PRGO12H (e) PRGONP (f) PRGOSIM

4. Conclusion

Graphene oxide was successfully synthesized from graphite flake using three selected methods – Hummers' method (with variation in oxidation time), modified Hummers' method without phosphoric acid and simplified Hummers' method. The FTIR results revealed that the intensity of C=O stretching vibration (1730 - 1740 cm^{-1}) peaks increased with time of oxidation from 11 hours to 12 hours but no significant changes were observed when time was increased from 12 hours upwards. The GOs synthesized using Hummers' method (GO11H, GO12H, GO13H and GO14) exhibited the highest level of oxidation followed by the one synthesized by simplified Hummers' method (GOSIM) and lastly the one by modified hummers' method without phosphoric acid (GONP). Raman spectra showed that the I_D/I_G ratio of all the GOs fell in the range 0.8-1.0. GOSIM showed the lowest value while GONP showed the highest value. Optical analysis showed that the signature n – π^* plasmon of the C=O bond occurred at 302 nm for all the GOs prepared by Hummers' method while it occurred at 309.48 nm and 308.56 nm for GO synthesized by simplified Hummers' method and modified hummers' method without phosphoric acid respectively. Consequently, in the case of Hummers' method, if the time of oxidation is increased beyond 12 hours, the effect may not be significant. GOs micrographs of all the variants revealed the formation of few sheets with folded edges, which are intercalated with roughed surfaces, due to structural deformation upon exfoliation and restacking. From the results obtained all the three methods used are capable of producing GO of different compositions. For modified Hummer's method, 12 hours of oxidation produce good result.

The variants of GOs (GO12H, GONP and GOSIM) were successfully reduced using two plants extracts (neem and pumpkin leaves) under room temperature. FTIR spectra of RGOs showed that the C=O signature of GOs at 1730 - 1740 cm^{-1} were eliminated after reduction. From the analysis of the Raman spectra, there was an increase in I_D/I_G ratio for all

the RGOs, which was attributed to the removal of oxygen and restoration of the sp^2 network. UV analysis revealed that, the π - π* plasmon peak of the C=C red-shifted to between258-265nm for RGOs. This was as a result of an increase in π - π* electron concentration and structural ordering. Also, the n - π* plasmon peak of the C=O bond red-shifted to between335 -350nm for RGOs as a result of reduction in sp^3 carbon. The results from SEM micrographs revealed that, after reduction, the folded edges were turned to sharp edges. With all these, the two plant extracts of neem and pumpkin are good reducing agents, which can replace the used of hazardous chemicals that are not ecofriendly.

Conflict of interest

On behalf of all authors, the corresponding author states that there is no conflict of interest.

Source of funding

This research did not receive any specific grant from funding agencies in the public, commercial, or not-for-profit sectors

References

[1] Alvial-Palavicino, C., & Konrad, K. (2019). The rise of graphene expectations: Anticipatory practices in emergent nanotechnologies. *Futures*, *109*, 192-202.

[2] Kostarelos, K. (2016). Translating graphene and 2D materials into medicine. *Nature Reviews Materials*, *1*(11), 1-2.

[3] Afroj, S., Tan, S., Abdelkader, A. M., Novoselov, K. S., & Karim, N. (2020). Highly conductive, scalable, and machine washable graphene-based E-textiles for multifunctional wearable electronic applications. Advanced Functional Materials, 30(23), 2000293.

[4] Su, H., Wu, T., Cui, D., Lin, X., Luo, X., Wang, Y., & Han, L. (2020). The Application of Graphene Derivatives in Perovskite Solar Cells. *Small Methods*, *4*(10), 2000507

[5] Jang, H., Park, Y. J., Chen, X., Das, T., Kim, M. S., Ahn, J. H. (2016). Graphene-based flexible and stretchable electronics. *Advanced Materials*, *28*(22), 4184-4202.

[6] Wang, B., Ruan, T., Chen, Y., Jin, F., Peng, L., Zhou, Y., ... & Dou, S. (2020). Graphene-based composites for electrochemical energy storage. Energy storage materials, 24, 22-51.

[7] Li, B., Luo, J., Huang, X., Lin, L., Wang, L., Hu, M., ... & Mai, Y. W. (2020). A highly stretchable, super-hydrophobic strain sensor based on polydopamine and graphene reinforced nanofiber composite for human motion monitoring. Composites Part B: Engineering, 181, 107580.

[8] Hummers Jr, W. S., Offeman, R. E. (1958). Preparation of graphitic oxide. *Journal of the American Chemical Society*, *80*(6), 1339-1339.

[9] Chen, J., Yao, B., Li, C., Shi, G. (2013). An improved Hummers method for eco-friendly synthesis of graphene oxide. *Carbon*, *64*, 225-229.

[10] Alam, S. N., Sharma, N., Kumar, L. (2017). Synthesis of graphene oxide (GO) by modified hummers method and its thermal reduction to obtain reduced grapheneoxide (rGO). *Graphene*, *6*(01), 1-18.

[11] Zaaba, N. I., Foo, K. L., Hashim, U., Tan, S. J., Liu, W. W., Voon, C. H. (2017). Synthesis of graphene oxide using modified hummers method:solventinfluence. *Procedia engineering*, *184*, 469-477.

[12] Guerrero-Contreras, J., Caballero-Briones, F. (2015). Graphene oxide powders with different oxidation degree, prepared by synthesis variations of the Hummers' method. *Materials Chemistry and Physics*, *153*, 209-220.

[13] Chong, S. W., Lai, C. W., Abd Hamid, S. B., Low, F. W., Liu, W. W. (2015).Simple preparation of exfoliated graphene oxide sheets via simplified Hummers' method. *Advanced Materials Research 1109*, 390-394.

[14] Liu, Y., Ma, J., Wu, T., Wang, X., Huang, G., Liu, Y., Qiu, H., Li, Y., Wang, W., Gao, J. (2013). Cost-effective reduced graphene oxide-coated polyurethane sponge as a highly efficient and reusable oil-absorbent. *ACS applied materials & interfaces*, *5*(20), 10018-10026.

[15] Longo, A., Palomba, M., and Carotenuto, G. (2020). Green Solid-State Chemical Reduction of Graphene Oxide Supported on a Paper Substrate. Coatings, 10(7), 693

[16] Eluyemi, M. S., Eleruja, M. A., Adedeji, A. V., Olofinjana, B., Fasakin, O., Akinwunmi, O. O., Ilori, O.O., Famojuro, A.T., Ayinde, S.A., Ajayi, E. O. B. (2016). Synthesis and characterization of graphene oxide and reduced graphene oxide thin films deposited by spray pyrolysis method. *Graphene*, *5*(3), 143-154.

[17] Faniyi, I. O., Fasakin, O., Olofinjana, B., Adekunle, A. S., Oluwasusi, T. V., Eleruja, M. A., Ajayi, E. O. B. (2019). The comparative analyses of reduced graphene oxide (RGO) prepared via green, mild and chemical approaches. *SN Applied Sciences*, *1*(10), 1181.

[18] Njoku, V. O., Obi, C. (2009). Phytochemical constituents of some selected medicinal plants. *African journal of pure and applied chemistry*, *3*(11), 228-233.

[19] Sithisarn, P., Muensaen, S., Jarikasem, S. (2011). Determination of Caffeoyl Quinic Acidsand Flavonoids in Acanthopanax Trifoliatus Leaves byHPLC. *Natural Product Communications*, *6*(9), 1289-1291.

[20] Saif, Z., Al-Hashemi, S., Hossain, M.A. (2016). Biological activities of different neem leaf crude extracts used locally in Ayurvedic medicine.*Pacific Science Review A: Natural Science and Engineering18* 128-131

[21] Roy, P., Periasamy, A. P., Chuang, C., Liou, Y. R., Chen, Y. F., Joly, J., Liang, C. T., Chang, H. T. (2014). Plant leaf-derived graphene quantum dots and applications for white LEDs. *New Journal of Chemistry*, *38*(10), 4946-4951.

[22] Aondona, I. P. (2018) Biosynthesis of Eco-Friendly Silver Nano-Particles using Dry Fluted Pumpkin (Telfairia occidentalis) Leave Extract as Reducing Agent.*Research & Development in Materials Science*, *4*(5), 432-436.

[23] Feng, M., & Feng, H. (2013). Effect of reducing agent on the chemical reduction of graphene oxides. Journal of nanoscience and nanotechnology, 13(2), 937-941.

[24] Wang, J., Salihi, E. C., & Šiller, L. (2017). Green reduction of graphene oxide using alanine. Materials Science and Engineering: C, 72, 1-6.

[25] Ciszewski, M., Mianowski, A. (2013). Survey of graphite oxidation methods using oxidizing mixtures in inorganic acids. *Chemik*, *67*(4), 267-274

[26] Picaud, S., Collignon, B., Hoang, P. N., Rayez, J. C. (2008). Adsorption of water molecules on partially oxidized graphite surfaces: a molecular dynamics study of the competition between OH and COOH sites. *Physical Chemistry Chemical Physics*, *10*(46), 6998-7009.

[27] Nguyen, V. T., Do, D. D., Nicholson, D. (2014). A new molecular model for water adsorption on graphitized carbon black. *Carbon*, *66*, 629-636.

[28] Dimiev, A.M.; Alemany, L.B.; Tour, J.M., (2013). Graphene oxide. Origin of acidity, its stability in water, and a new dynamic structural model. *ACS Nano*, *7* (1), 576-588

[29] Dimiev, A. M., Eigler, S. (Eds.). (2016). *Graphene oxide: fundamentals and applications*. John Wiley and Sons. Page 96

[30] Dubale, A. A., Su, W. N., Tamirat, A. G., Pan, C. J., Aragaw, B. A., Chen, H.M., Chen, C. H., Hwang, B. J. (2014). The synergetic effect of graphene on Cu_2O nanowire arrays as a highlyefficient hydrogen evolution photocathode in water splitting. *J. Mater. Chem. A*, *2*, 18383-18397

[31] Cancado, L. G., Jorio, A., Martins-Ferreira, E. H., Stavale, F., Achete, C. A., Capaz, R. B., Montinho, M. v. O., Lombardo, A., Kulmala, T. S., Frrari, A. C. (2011). Quantifying defects in graphene via Raman spectroscopy at different excitation energies. *Nano Letters*, *11*, 3190-3196.

[32] Fan, H., Zhang, T., Xu, X., Lu, N. (2011). Fabrication of N-type Fe_2O_3 and P-type $LaFeO_3$ Nanobelts by Electrospinning and Determination of Gas-Sensing Properties. *Sensorsand Actuators B: Chemical*, *153*(1), 83-88.

[33] Kudin, K. N., Ozbas, B., Schniepp, H. C., Prud'Homme, R. K., Aksay, I. A., Car, R. (2008). Raman Spectra of Graphite Oxide and Functionalized Graphene Sheets. *Nano Letters*, *8*(1), 36-41.

[34] Zickler, G. A., Smarsly, B., Gierlinger, N., Peterlik, H.,Paris, O. (2006). A Reconsideration of the Relationship Between the crystallite size La of CarbonsDetermined by X-ray Diffraction and Raman Spectroscopy. *Carbon*, *44*(15), 3239-3246.

[35] Tuinstra, F., Koenig, J. L. (1970). Characterization of graphite fiber surfaces with Raman spectroscopy. *Journal of Composite Materials*, *4*(4), 492-499.

[36] Cançado, L. G., Takai, K., Enoki, T., Endo, M., Kim, Y. A., Mizusaki, H., Jorio, A., Coelho, L. N., MagalhaesPaniago, R., Pimenta, M.A. (2006). General equation for the

determination of the crystallite size L_a ofnanographite by Raman spectroscopy. *Applied Physics Letters*, *88*(16), 163106.

[37] Abakumov, A. A., Bychko, I. B., Nikolenko, A. S., Strizhak, P. E. (2018). Dependence of Structure of Multilayer Graphene Oxide on Degree of Graphitization ofInitial Graphite. *Theoretical and Experimental Chemistry*, *54*(3), 186 -192

[38] Banhart, F., Kotakoski, J., Krasheninnikov, A. V. (2010). Structural Defects in Graphene. *ACS Nano*, *5*(1), 26-41.

[39] Saini, P., Sharma, R., Chadha, N. (2017). Determination of Defect Density,Crystallite Size and Number of Graphene Layers in Graphene Analogues Using X-ray Diffraction and Raman Spectroscopy. *Indian Journal of Pure and Applied Physics (IJPAP)*, *55*(9),625-629.

[40] Yang, C. R., Tseng, S. F.,Chen, Y. T. (2018). Characteristics of graphene oxide films reduced by using an atmospheric plasma system. *Nanomaterials*, *8*(10), 802.

[41] Luo, Z., Vora, P. M., Mele, E. J., Johnson, A. C., Kikkawa, J. M. (2009). Photoluminescence and Band Gap Modulation in Graphene Oxide. *Applied Physics Letters*, *94*(11), 111909.

[42] Cao, J., Emadi, A. (2012). A New Battery/Ultracapacitor Hybrid Energy Storage Systemfor Electric, Hybrid, and Plug-in Hybrid Electric Vehicles. *IEEE Transactions on Power Electronics*, *27*(1), 122-132.

[43] Badenhorst, H. (2017). Graphite Oxidation and SEM as a Tool for Microstructural Investigation. *Transactions of the Royal Society of South Africa*, *72*(3), 294-300.

[44] Gurunathan, S., Jae W. H., Vasuki., Ahmed A. D., Kwon D-N.,Kim J-H., (2013). Biocompatibility effects of biologically synthesized graphene in primary mouse embryonic fibroblast cells. *Nanoscale Research Letters*, 8, 393, 1-13.

[45] Olumurewa, K. O., Olofinjana, B., Fasakin, O., Eleruja, M. A., Ajayi, E. O. B. (2017). Characterization of high yield graphene oxide synthesized by simplified hummers' method. *Graphene*, *6*(4), 85-98.

[46] Yousefi, N., Gudarzi, M.M., Zheng, Q., Aboutalebi, S. H., Sarif, F., Kim, J. K. (2012). Self-alignment and high electrical conductivity of ultralarge graphene oxide-polyurethane nanocomposites. *Journal of Materials Chemistry*, *22*, 12709-12717.

[47] Bonaccorso, F., Lombardo, A., Hasan, T., Sun, Z., Colombo, L., Ferrari, A. C. (2012). Production and processing of graphene and 2d crystals. *Materials Today*, *15*(12),564-589.

[48] Hareesh K, Joshi R P, Dahiwale S S, BhoraskarVNand Dhole SD2016 Synthesis of Ag-reduced graphene oxide nanocomposite by gamma rays Vacuum 124 40–5

[49] Stankovich S, DikinDA, Piner RD, KohlhaasKA, Kleinhammes A, Jia Y, Yue W, Nguyen S T and Ruoff R S 2007 Synthesis of graphene-based Nanosheets via chemical reduction of exfoliated graphite oxide Carbon 45 1558–65

[50] Grzegorz S, Jaroslaw S, Joanna J, Rafal K, Mariusz Z, Marcin H, Piotr P, Jakub B, Ludwika L and KrzysztofMA2012 Graphene oxide vs. reduced graphene oxide as saturable absorbers for Er-Doped passively Mode-Locked fiber laser Opt. Express 20 19463–73

[51] Olumurewa, K. O., Olofinjana, B., Fasakin, O., Akhigbe, G. E., Eleruja, M. A., & Ajayi, E. O. B. (2020). Effect of hydrothermal and chemical treatment on the optical and electrical properties of reduced graphene oxide deposited on ITO glass. Materials Research Express, 7(10), 105606.

[52] Eigler, S. (2014). Mechanistic insights into the reduction of graphene oxide addressing itssurfaces. *Phys. Chem. Chem. Phys.16* (37), 19832–19835.

[53] Ferrari, A. C. (2007). Raman spectroscopy of graphene and graphite: disorder, electron–phonon coupling, doping and nonadiabatic effects. *Solid state communications*, *143*(1-2), 47-57.

[54] Xu, C., Shi, X., Ji, A., Shi, L., Zhou, C., Cui, Y. (2015). Fabrication and characteristics of reduced graphene oxide produced with different green reductants. *PloSONE*, *10*(12) 0144842.

[55] Eda, G., Chhowalla, M. (2010). Chemically Derived Graphene Oxide: Towards Large-Area Thin-Film Electronics and Optoelectronics. *Advanced Materials*, *22*(22), 2392-2415.

[56] Wong, C. P. P., Lai, C. W., Lee, K. M., & Hamid, S. B. A. (2015). Advanced chemical reduction of reduced graphene oxide and its photocatalytic activity in degrading reactive black 5. *Materials*, *8*(10), 7118-7128.